ADA027577

(2)

FC

Nonlinear Scaling Laws for Parametric Receiving Arrays

Part I Theoretical Analysis

prepared under:

Contract N00039-75-C-0259 NEW
ARPA Order 2910
Program Code 5G10

Authors:

F. H. Fenlon — Applied Research Laboratory, Pennsylvania State University, State College, Pennsylvania

J. W. Kesner — Westinghouse Electric Corporation, Oceanic Division, Annapolis, Maryland

June 30, 1976

Westinghouse Electric Corporation
Oceanic Division
P. O. Box 1488
Annapolis, Maryland 21404

6

Nonlinear Scaling Laws for Parametric Receiving Arrays.

Part I. Theoretical Analysis,

prepared under:

15

~~Contract~~ N00039-75-C-0259
ARPA Order-2910
Program Code 5G10

Authors:

10

F. H. Fenlon

Applied Research Laboratory
Pennsylvania State University
State College, Pennsylvania

J. W. Kesner

Westinghouse Electric Corporation
Oceanic Division
Annapolis, Maryland

11 30 June ~~30,~~ 1976

12 48p.

Westinghouse ~~Electric Corporation~~
Oceanic Division
P. O. Box 1488
Annapolis, Maryland 21404

407381

LB

List of Symbols

v, v_o	particle velocity and its peak value at the source, respectively
u_s, u_p	signal and pump fields, respectively
u_ω, u_n	continuous and discrete spectral forms of u, respectively
ψ_n	axial component of u_n
ψ_n^o, $\bar{\psi}_n^o$, $\hat{\psi}_n^o$	zero-order Laguerre mode, and real, imaginary parts, respectively
c_o	small signal speed of sound
β	nonlinear parameter (e.g., $\beta = \frac{\gamma + 1}{2}$ in gases where $\gamma = c_p/c_v$ $= 1 + \frac{B}{2A}$ in liquids)
$\varepsilon_o = u_o/c_o$	Peak Mach Number
ω_o	angular frequency of a pure tone radiated by the source (e.g., pump wave)
Ω	angular frequency of a signal in the medium
$N = \omega_o/\Omega$	'frequency up-shift' ratio
x, y, z, t	space-time coordinates
a	radius of a circular piston projector
$r_o = k_o a^2/2$	piston projector Rayleigh distance
$\xi = (x^2+y^2)/a^2$	normalized off-axis coordinate
$\tau = \Omega(t-z/c_o)$	nondimensional retarded time coordinate
$R = z/r_o$	normalized range coordinate
$\sigma_o = \beta\varepsilon_o k_o r_o$, $\sigma_\Omega = \beta\varepsilon_o k_\Omega r_o$	scaled source tone and signal parameters, respectively
$\sigma = \sigma_o F(R)$	'stretched' range coordinate (e.g., $F(R) = \sinh^{-1} R$ for a plane piston projector)
α_ω, α_Ω	thermo-viscous attenuation coefficients at angular frequencies ω and Ω, respectively
k_ω, k_Ω	wavenumbers at angular frequencies ω and Ω, respectively
L_k	Laguerre Polynomial of order k

H_o, Y_o	zero order Struve and Neumann functions, respectively
$X_\Omega = k_\Omega - i\alpha_\Omega$	complex wavenumber at angular frequency Ω
Θ	angle of intersection between signal and pump wave normals
$p'_\pm/p'_{s_o}$	signal excess
$D_\pm(\Theta)$	up-converted directivity functions
$Jm(x)$	Bessel Function of order m

Figure Captions

Figure 1. Axial Pressure Field of a 454 kHz Signal Radiated by a 3" Diameter Projector in Fresh Water [$r_o = 1.5$ yds, $\alpha_1 r_o = 7.35 \times 10^{-3}$ Np, B/A = 4.9].

Figure 2a. Axial Pressure Field of a 454 kHz Signal in Fresh Water.

Figure 2b. Axial Pressure Field for the Second Harmonic of a 454 kHz Signal Generated Via Nonlinear Self-Interaction of the Fundamental in Fresh Water.

Figure 3. Finite-Amplitude Absorption Losses Incurred by a 454 kHz Signal in Fresh Water.

Figure 4. Far-Field Finite-Amplitude Absorption Characteristics

$$[20 \operatorname{Log}_{10}\sigma_o = SL_o + 20 \operatorname{Log}_{10} (\sqrt{2}\,\beta k_o/\rho_o c_o^2)$$
$$\equiv SL_o^* + 20 \operatorname{Log}_{10}(2\pi\sqrt{2}\,\beta \times 10^{-3}/\rho_o c_o^3) = SL_o^* - 180 \text{ dB}$$

in water (1 μbar = reference pressure)

where $SL_o = 20 \operatorname{Log}(p_o r_o/\sqrt{2})$

and $SL_o^* = 20 \operatorname{Log}(p_o r_o f_o/\sqrt{2})$; f_o in kHz].

Figure 5a. Signal-Excess Characteristics

Figure 5b. Up-Converted Directivity Characteristics

Figure 6. Approximate Signal-Excess Characteristics

Abstract

Following a review of the literature on Parametric Receiving Arrays, the problem of defining their performance characteristics under saturated and unsaturated conditions is considered. Basically, the problem is resolved by establishing equations for the axial field of a spatially symmetric pump wave in the spectral domain via Kuznetsov's nonlinear paraxial wave equation. As a biproduct of this analysis, a simplification of terms involving the phase of pump wave in these equations results, upon transformation to the time domain, in a new form of Burgers' equation for a plane piston projector. Unlike previous forms of Burgers' equation, the latter combines the effect of wave interactions in the near and far field regions of the source. Numerical comparisons of the more complete spectral equations and the spectral form of the new Burgers' equation are shown to be in good agreement with experimental results previously reported in the literature. Approximate solutions of these equations are also derived. The three methods thus established for representing the pump field are then used to derive scaling laws for parametric receiving arrays, which clearly show the limiting effect of pump wave saturation upon the conversion efficiency of the up-conversion process as the pump amplitude is increased indefinitely.

Introduction

In his work on the scattering-of-sound-by-sound, Westervelt[1,2] concluded that two overlapping perfectly collinated plane waves of finite-amplitude would only give rise to scattered waves when propagating in the same direction - a result in keeping with the anharmonic resonance conditions discussed by Landau and Lifshitz.[3] This work led naturally to his fundamental paper on the Parametric Array where Westervelt[4] deduced that two perfectly collinated coterminous progressive finite-amplitude plane waves of angular frequencies ω_1 and ω_2 traveling in the same direction in an unbounded nondispersive fluid medium would interact to produce highly directive intermodulation spectral components; that of frequency $\omega_1 - \omega_2$, referred to as the "difference-frequency signal" being the lowest in the spectrum. Since he was primarily interested in the generation of low frequency waves, Westervelt's[4] analysis required that the primary frequencies be very nearly equal. This requirement, which makes possible the process of frequency "down-conversion," is basic to parametric transmitting arrays, although of course upper sideband components are also formed.

Alternatively, when viewed analytically, simultaneous radiation by the source of frequencies ω_1 and ω_2 with equal finite-amplitudes is equivalent to sinusoidal modulation of a finite-amplitude carrier wave or "pump" wave of frequency $\omega_o = \frac{1}{2}(\omega_1 + \omega_2)$ by a signal of frequency $\Omega/2$, where $\Omega = \omega_1 - \omega_2$. It follows therefore, from the inherent "quadratic" nonlinearity of the medium that the spectral components of the modulating envelope squared and in particular the difference-frequency Ω, will be amplified or "pumped" at the expense of the carrier until the amplitude of the latter is reduced by this and other absorption losses to a level where

it can no longer sustain a nonlinear interaction. The reader should note at this point that the interaction is not confined to suppressed carrier modulation, as exemplified by the work of Eller[5] and Merklinger[6] on more general forms of modulation. Viewed in this manner however, it is clear that the process of parametric amplification can be interpreted in terms of the concept of finite-amplitude self-demodulation introduced by Berktay[7] and justified experimentally by Moffett, Westervelt, and Beyer.[8]

Likewise, in the converse process of frequency "up-conversion," parametric receiving arrays are formed by projecting a finite-amplitude pump wave of angular frequency ω_o into the medium to serve as the carrier wave for a weak incoming signal of frequency Ω, where $\omega_o/\Omega >> 1$. In this instance the pump field is augmented by the spatial component of the signal along the pump axis, assuming of course, that both the pump wave and this component are traveling in the same direction. The resulting nonlinear interaction gives rise to an intermodulation spectrum as before, the sum and difference frequency components $\omega_o \pm \Omega$ being of greatest interest. Since ω_o/Ω is assumed to be considerably greater than unity however, these sidebands are now in close spectral proximity to the pump frequency, but unlike the latter their directivity is equivalent to that of a virtual-end-fire line array of length L/λ_Ω (in wavelengths of the signal frequency) where L is the distance from the pump projector along its axis at which a receiving hydrophone resonant at $\omega_o + \Omega$ or $\omega_o - \Omega$ is located. Upon reception the "up-converted" signal is fed to a low pass filter to remove the pump frequency and recover the signal of frequency Ω.

Although implicit in Westervelt's work,[1,2,4] the process of Parametric reception was identified and made explicit by the extensive theoretical and experimental investigations of Berktay[9] who in cooperation with Al-Temimi[10-12] considered the practical implications of the up-conversion process. Subsequent experimental work[13,14] has been directed to long wavelength up-conversion in fresh water lakes[13] and to the consideration of arrays of parametric receivers,[14] thus involving significant practical extensions of the original scaled laboratory experiments. Further theoretical extensions[15,16] have also been made to provide a more precise description of the pump fields radiated by practical sources and the resulting effect of such refinements upon the analytical form of solutions for the up-converted fields. More recently Goldsberry[17] and McDonough[18] have derived optimum operating conditions for parametric receiving arrays from systems analyses based on Berktay and Al-Temimi's analytical model[10] for a spherically spreading pump wave. With the exception of a preliminary study by Bartram[19] there has been no systematic study of the effect of finite-amplitude absorption on the performance of parametric receivers, which although insignificant at low pump amplitudes, ultimately determines the maximum achievable efficiency of these arrays when the pump wave becomes saturated. In order to provide a more complete analysis of this effect we now consider how Kuznetsov's[20] nonlinear paraxial wave equation (which on account of its parabolic form is ideally suited to numerical solution) can be used to define the acoustic field of a pump wave radiated by a plane piston projector under both saturated and unsaturated conditions. Following this analysis we will then determine the effect of saturated pump waves on the conversion efficiency of parametric receiving arrays, and hence deduce scaling laws to define their performance capabilities.

1. Kuznetsov's Equation

In this section we wish to investigate the distortion of progressive finite-amplitude waves in an unbounded nondispersive fluid via Kuznetsov's[20] nonlinear paraxial wave equation, which it should be noted, is a more general form of the inviscid paraxial wave equation previously derived by Zabolotskaya and Khokhlov.[21,22] Introducing a rectilinear Cartesian coordinate system and considering the propagation of progressive plane finite-amplitude waves along the positive z axis, Kuznetsov's[20] equation can be expressed as,

$$\frac{\partial^2 u}{\partial\tau\partial z} - (1/2\ k_\Omega)\nabla^2_{xy}u = \frac{\partial}{\partial\tau}\left\{(\beta\varepsilon_o k_\Omega)u\frac{\partial u}{\partial\tau} + \alpha_\Omega\frac{\partial^2 u}{\partial\tau^2}\right\} \tag{1}$$

where

$$u = v/v_o\ , \quad \varepsilon_o = v_o/c_o\ , \quad k_\Omega = \Omega/c_o\ , \quad \tau = \Omega(t - \frac{z}{c_o}) \tag{2}$$

and

$$\nabla^2_{xy} \equiv \frac{\partial^2}{\partial x^2} + \frac{\partial^2}{\partial y^2}\ . \tag{3}$$

In this notation v denotes the particle velocity resulting from propagation of an acoustic disturbance in the fluid, v_o being its peak value at the source; ρ_o is the static density, c_o is the small-signal speed-of-sound, ε_o is the peak Mach number at the source, and β is the second-order nonlinear coefficient of the fluid; Ω is an, as yet unspecified, angular frequency, and α_Ω is the corresponding small-signal thermo-viscous attenuation coefficient.

Assuming that an axially symmetric disturbance is established in the field via radiation from a baffled piston source of radius a , it is convenient to normalize the variables x and y with respect to a and combine them in a single variable ξ defined by Rudenko, Soluyan, and Khokhlov[23] as,

$$\xi = (x/a)^2 + (y/a)^2 \quad . \tag{4}$$

Expressing the x and y derivatives in terms of ξ we obtain,

$$\frac{\partial}{\partial x} = \frac{\partial \xi}{\partial x} \frac{\partial}{\partial \xi} \ , \qquad \frac{\partial}{\partial y} = \frac{\partial \xi}{\partial y} \frac{\partial}{\partial \xi}$$

hence, from Equations (3) and (4),

$$\nabla^2_{xy} = \left(\frac{\partial \xi}{\partial x} \frac{\partial}{\partial \xi} \right)^2 + \left(\frac{\partial \xi}{\partial y} \frac{\partial}{\partial \xi} \right)^2$$

$$= \left(\frac{2}{a} \right)^2 \frac{\partial}{\partial \xi} \left(\xi \frac{\partial}{\partial \xi} \right) \quad . \tag{5}$$

Substituting Equation (5) in Equation (1) thus gives,

$$\frac{\partial^2 u}{\partial \tau \partial z} - (k_\Omega a^2/2)^{-1} \frac{\partial}{\partial \xi} (\xi \frac{\partial u}{\partial \xi}) = \frac{\partial}{\partial \tau} \left\{ (\beta \varepsilon_o k_\Omega) u \frac{\partial u}{\partial \tau} + \alpha_\Omega \frac{\partial^2 u}{\partial \tau^2} \right\} \quad . \tag{6}$$

Normalizing z with respect to a reference 'Rayleigh distance' $r_o = k_o a^2/2$ where $k_o = \omega_o/c_o$, and the, as yet unspecified frequency ω_o is assumed to be radiated directly by the source, Equation (6) becomes,

$$\frac{\partial^2 u}{\partial \tau \partial R} - \left(\frac{\omega_o}{\Omega} \right) \frac{\partial}{\partial \xi} \left[\xi \frac{\partial u}{\partial \xi} \right] = \frac{\partial}{\partial \tau} \left\{ \sigma_\Omega u \frac{\partial u}{\partial \tau} + (\alpha_\Omega r_o) \frac{\partial^2 u}{\partial \tau^2} \right\} \tag{7}$$

where $R = z/r_o$, $r_o = k_o a^2/2$, $k_o = \omega_o/c_o$, $\sigma_\Omega = \beta \varepsilon_o k_\Omega r_o$. (8)

Alternatively, in terms of the 'stretched coordinate system' introduced by Blackstock,[24] Equation (7) becomes,

$$\frac{\partial^2 u}{\partial\tau\partial\sigma} - (1/\sigma_o)\frac{\partial}{\partial\xi}\left[\xi\frac{\partial u}{\sigma\xi}\right] = \frac{\partial}{\partial\tau}\left\{u\frac{\partial u}{\partial\tau} + (\Omega/\omega_o)^2\,\Gamma_o^{-1}\frac{\partial^2 u}{\partial\tau^2}\right\} \tag{9}$$

where

$\sigma_o = \beta\varepsilon_o k_o r_o$, $\sigma = \sigma_o R$, and $\Gamma_o = \sigma_o/\alpha_o r_o$ is the Acoustic Reynolds number. (10)

It is clear from inspection of Equations (7) and (9) that for one dimensional waves they reduce to the plane wave form of Burgers' equation.[24,25]

Returning to Equation (7) and expressing u in terms of its Fourier transform u_ω we obtain,

$$\frac{\partial u_\omega}{\partial R} + i\left(\frac{\omega_o}{\omega}\right)\frac{\partial}{\partial\xi}\left[\xi\frac{\partial u_\omega}{\partial\xi}\right] + (\alpha_\omega r_o)u_\omega = i\left(\frac{\omega}{\Omega}\right)\left(\frac{\sigma_\Omega}{2}\right)(u_\omega * u_\omega) \tag{11}$$

where

$$u_\omega(R,\xi) = \int_{-\infty}^{\infty} u(R,\xi,\tau')e^{-i(\omega/\Omega)\tau'}d\tau' \tag{12a}$$

$$u(R,\xi,\tau) = \frac{1}{2\pi}\int_{-\infty}^{\infty} u_\omega(R,\xi)e^{i(\omega/\Omega)\tau}d(\omega/\Omega) \tag{12b}$$

$$u_\omega * u_\omega = \frac{1}{2\pi}\int_{-\infty}^{\infty} u_{\omega-\omega'}u_{\omega'}\,d(\omega'/\Omega) \tag{12c}$$

and

$$\alpha_\omega = \alpha_\Omega(\omega/\Omega)^2 \quad . \tag{12d}$$

If the signal of angular frequency ω_o radiated by the source is sinusoidally modulated by a pure tone of angular frequency Ω then for integral values of $N = \omega_o/\Omega \geq 1$, ω assumes the discrete values $\omega_n = n\Omega$ and Equation (11) becomes the infinitely coupled set of partial differential equations given by,

$$\frac{\partial u_n}{\partial R} + i\left(\frac{N}{n}\right)\frac{\partial}{\partial \xi}\left(\xi \frac{\partial u_n}{\partial \xi}\right) + (\alpha_n r_o)u_n = i\left(\frac{n}{N}\right)\left(\frac{\sigma_o}{2}\right)\sum_{m=-\infty}^{\infty} u_{n-m}u_m$$

$$= i\left(\frac{n}{N}\right)\left(\frac{\sigma_o}{2}\right)\left\{\sum_{m=1}^{n-1} u_{n-n}u_m + 2\sum_{m=1}^{\infty} u_{n+m}u_m^*\right\} \tag{13}$$

where u_m^* , denoting the complex conjugate of u_m , appears in Equation (13) because $u(R,\xi,\tau)$ is a real valued function and consequently $u_{-m} \equiv u_m^*$ from Equation (12a). Obviously, if the source waveform is unmodulated, we simply set $N = 1$.

At this point we note that since the left-hand-side of Equation (13) is similar to the time dependent form of Schrödinger's equation, we can express the axially symmetric spectral amplitudes $u_n(R,\xi)$ as a Laguerre polynomial expansion given by,

$$u_n(R,\xi) = e^{-(n/N)\xi/1 - iR} \sum_{k=0}^{\infty} \frac{1}{2}\psi_n^k(R)L_k(\xi) \tag{14}$$

where the Laguerre polynomials $L_k(\xi)$ obey the following relationships,[26]

$$\int_o^{\infty} e^{-\xi}L_k(\xi)L_\ell(\xi)d\xi = \begin{cases} (k!)^2, & k = \ell \\ 0 \ , & k \neq \ell \end{cases} \tag{15a}$$

$$L_k'(\xi) - kL_{k-1}'(\xi) = -kL_{k-1}(\xi) \tag{15b}$$

$$\xi L'_k(\xi) - kL_k(\xi) = -k^2L_{k-1}(\xi) \tag{15c}$$

$$L_o(\xi) = 1 \ ; \quad L_1(\xi) = -\xi + 1 \ ; \quad L_2(\xi) = \xi^2 - 4\xi + 2 \ , \text{ etc.} \tag{15d}$$

Substituting Equation (14) in Equation (13) and employing Equations (15a) through (15c) to simplify the resulting expressions, we obtain after some manipulation,

$$\frac{d\psi_n^k}{dR} + \left[\alpha_n r_o - \frac{i(1+k)}{1-iR}\right]\psi_n^k = i\left(\frac{n}{N}\right)\left(\frac{\sigma_o}{4}\right)\left\{\sum_{m=1}^{n-1}\sum_{s,\ell=0}^{\infty}\sum A_{s\ell}^k\psi_{n-m}^s\psi_m^\ell\right.$$

$$\left. + 2\sum_{m=1}^{\infty}\sum_{s,\ell=0}^{\infty}\sum B_{s\ell}^k\psi_{n+m}^s\psi_m^{\ell^*}\right\} \tag{16}$$

where

$$A_{s\ell}^k = \left(\frac{1}{k!}\right)^2\int_o^\infty e^{-\xi}\,L_k(\xi)L_s(\xi)L_\ell(\xi)d\xi \tag{17a}$$

and

$$B_{s\ell}^k = \left(\frac{1}{k!}\right)^2\int_o^\infty e^{-\xi\left(1+\frac{2m/N}{1+R^2}\right)}L_k(\xi)L_s(\xi)L_\ell(\xi)d\xi \quad . \tag{17b}$$

In order to solve Equation (16), we require the initial values $\psi_n^k(0)$. These can be obtained from Equation (14) if the boundary value $u_n(0,\xi)$ is prescribed. Thus, by means of the orthogonal relationship defined by Equation (15a) we have,

$$\psi_n^k(0) = \left(\frac{1}{k!}\right)^2\int_o^\infty e^{-\xi(1-n/N)}\,u_n(0,\xi)L_k(\xi)d\xi \quad . \tag{18}$$

If, for example, $u_n(0,\xi) = 1, \quad 0 \le \xi \le 1$

$$= 0, \quad \xi > 1 \tag{19}$$

and $N = 1$ then,

$$\psi_n^k(0) = \left(\frac{k-1}{n-1}\right)\left\{L_{k-1}(0) - e^{n-1}L_{k-1}(1)\right\} + \left(\frac{kn}{n-1}\right)\psi_n^{k-1}(0) \;;$$

$$n,\ k > 1 \tag{20a}$$

where

$$\psi_1^k(0) = \int_0^1 L_k(\xi)d\xi \tag{20b}$$

and

$$\psi_n^o(0) = \left(\frac{1}{n-1}\right)\left\{e^{n-1} - 1\right\}, \quad n > 1 \;; \quad \psi_1^o(0) = 1 \quad . \tag{20c}$$

In general, the tripple sums on the right-hand-side of Equat' .. (16) are very difficult to evaluate, particularly as Equations (17a) and (17b) cannot be reduced to simple closed form expressions if k, s, ℓ are non zero. For any value of k however, since the largest terms in the double summation over s and ℓ are those for which $s = \ell$, we can neglect the terms $s \neq \ell$ over small increments of the distortion distance $\sigma_o F(R)$, where $F(R)$ is a function which has yet to be defined. Moreover, since the field is most intense along the beam axis, the particular values $s = \ell = 0$ are dominant, thus giving the resulting approximation to Equation (16), valid for small values of $\sigma_o F(R)$,

$$\frac{d\psi_n^k}{dR} + \left(\alpha_n r_o - \frac{i(1+k)}{1-iR}\right)\psi_n^k = i\left(\frac{n}{N}\right)\left(\frac{\sigma_o}{4}\right)\left\{A_{oo}^k \sum_{m=1}^{n-1} \psi_{n-m}^o \psi_m^o + 2\sum_{m=1}^{\infty} B_{oo}^k(m)\psi_{n+m}^o \psi_m^{o*}\right\} \tag{21}$$

where

$$A_{oo}^k = \left(\frac{1}{k!}\right)^2 \int^{\infty} e^{-\xi} L_k(\xi)\,d\xi \;, \qquad A_{oo}^o = 1 \tag{22a}$$

and

$$B_{oo}^k(m) = \left(\frac{1}{k!}\right)^2 \int^{\infty} e^{-\xi\left(1 + \frac{2m/N}{1+R^2}\right)} L_k(\xi)\,d\xi \;, \qquad B_{oo}^o(m) = \frac{1}{1 + \frac{2m/N}{1+R^2}} \tag{22b}$$

Inspection of Equation (21) shows that the zero order Laguerre mode (i.e. $k = 0$) is now independent of the higher order modes (i.e. $k = 1,2, \ldots$), which can all be derived from it a-posteriori. Physically, this implies that the axial field is predominantly defined by the zero order Laguerre mode, which in turn is primarily responsible for distortion of the off-axis field, the latter having little effect on the axial field over small distortion distances.

Furthermore, since small increments of the 'scaled' range $\sigma_o F(R)$ imply large increments in actual range R for $\sigma_o << 1$, the model ensures that all Laguerre modes other than zero will be insignificantly small under <u>unsaturated</u> conditions. Thus, for a monofrequency source (i.e. $N = 1$) the <u>unsaturated</u> harmonic directivity functions formed by self interaction of the fundamental frequency component in the medium are given by Equation (14) as Gaussian beam patterns,

$$D_n(R,\xi) = \left\{ e^{-n\xi(1 - iR)/(1 + R^2)} \right\} \left\{ e^{-n\xi(1 - iR)/(1 + R^2)} \right\}^*$$

$$= e^{-2n\xi/(1 + R^2)} \tag{23a}$$

$$\rightarrow e^{-2n\xi/R^2} = e^{-\frac{n}{2}(k_o a \sin\theta)^2} , \quad R >> 1 . \tag{23b}$$

Thus, in keeping with Rudenko, Soluyan and Khokhlov's investigation,[23] the model is capable of defining the major lobe, but not the minor lobe structure of the actual field. Under <u>saturated</u> conditions as more and more higher-order Laguerre modes are included in Equation (14), the harmonic directivity functions become,

$$D_n(R,\xi) = \left| \frac{u_n(R,\xi)u_n^*(R,\xi)}{u_n(R,0)u_n^*(R,0)} \right|$$

$$= \left| 1 + \frac{\sum\sum_{k,\ell=1}^{\infty} \psi_n^k(R)\psi_n^{\ell^*}(R)L_k(\xi)L_\ell(\xi)}{\sum\sum_{k,\ell=1}^{\infty} \psi_n^k(R)\psi_n^{\ell^*}(R)L_k(0)L_\ell(0)} \right| e^{-2n\xi/(1 + R^2)} . \tag{24}$$

Under unsaturated conditions, $\psi_n^k \to 0$ for $k \neq 0$, so that Equation (24) reduces to the form of Equation (23) as required. With increasing values of σ_o therefore, as the number of terms in the summations of Equation (24) increase, the directivity functions should broaden in accordance with the experimental results of Shooter, Muir and Blackstock.[27]

Since the zero-order Laguerre mode can be evaluated independently of the higher order modes for the model under consideration, it is expedient to consider the differential equations for this mode alone. These are given by Equation (21) as

$$\frac{d\psi_n^o}{dR} + \left(\alpha_n r_o - \frac{i}{1 - iR}\right)\psi_n^o = i\left(\frac{n}{N}\right)\left(\frac{\sigma_o}{4}\right)\left\{\sum_{m=1}^{n-1} \psi_{n-m}^o \psi_m^o + 2\sum_{m=1}^{\infty}\left(\frac{1}{1 + \frac{2m/N}{1 + R^2}}\right)\psi_{n+m}^o \psi_m^{o*}\right\} . \tag{25}$$

In Appendix A it is shown that under unsaturated conditions the second harmonic field in an inviscid fluid obtained from Equation (25) by the method of successive approximations is identical as $\alpha_1 r_o \to 0$ to the approximate solution previously derived from the inviscid form of Equation (9) by Rudenko, Soluyan and Khokhlov.[23]

Since ψ_n^o is complex it is convenient to express it in terms of its real and imaginary parts $\overline{\psi}_n^o$ and $\hat{\psi}_n^o$ respectively where,

$$\psi_n^o = \overline{\psi}_n^o - i\hat{\psi}_n^o \quad ; \qquad \overline{\psi}_{-n}^o = \overline{\psi}_n^o \quad , \qquad \hat{\psi}_{-n}^o = -\hat{\psi}_n^o \quad . \tag{26}$$

Substituting Equation (26) in Equation (25) and equating the real and imaginary terms respectively we thus obtain,

$$\frac{d}{dR}\begin{pmatrix}\bar{\psi}^o_n \\ \hat{\psi}^o_n\end{pmatrix} + (\alpha_n r_o)\begin{pmatrix}\bar{\psi}^o_n \\ \hat{\psi}^o_n\end{pmatrix} + \left(\frac{1}{1+R^2}\right)\begin{pmatrix} R & -1 \\ 1 & R\end{pmatrix}\begin{pmatrix}\bar{\psi}^o_n \\ \hat{\psi}^o_n\end{pmatrix}$$

$$= \left(\frac{n}{N}\right)\left(\frac{\sigma_o}{4}\right)\sum_{m=1}^{n-1}\begin{pmatrix}\hat{\psi}^o_{n-m} & \bar{\psi}^o_{n-m} \\ -\bar{\psi}^o_{n-m} & \hat{\psi}^o_{n-m}\end{pmatrix}\begin{pmatrix}\bar{\psi}^o_m \\ \hat{\psi}^o_m\end{pmatrix}$$

$$+ \left(\frac{n}{N}\right)\left(\frac{\sigma_o}{2}\right)\sum_{m=1}^{\infty}\left(\frac{1}{1+\frac{2m/N}{1+R^2}}\right)\begin{pmatrix}\hat{\psi}^o_{n+m} & -\bar{\psi}^o_{n+m} \\ -\bar{\psi}^o_{n+m} & -\hat{\psi}^o_{n+m}\end{pmatrix}\begin{pmatrix}\bar{\psi}^o_m \\ \hat{\psi}^o_m\end{pmatrix} \qquad (27)$$

With the exception of the "diffraction-induced spreading losses" on the left-hand-side of Equation (27) and the coefficient $\left(1/1 + \frac{2m/N}{1+R^2}\right)$ in the summation on the right-hand-side, the coupled harmonic modes are similar to those previously considered by Bellman, Azen and Richardson[28] in their numerical analysis of the plane wave form of Burgers' equation. Solving these equations for a monofrequency source (i.e. N = 1) by a predictor-corrector method of the Adams Moulton type,[29] we examined, among other cases, the experiment conducted by Shooter, Muir and Blackstock.[27] In this instance a 3" diameter plane piston projector operating at 454 kHz in fresh water at 17.8°F was driven at source levels from 100-135 dB re 1 μbar at 1 yd. Assuming the same parameters as those previously chosen,[27] we have $\alpha_1/f^2 = 2.6 \times 10^{-14}$ Np/m at 17.8°F, $r_o = 1.5$ yds, and $B/A = 4.9$; consequently, we obtain $\alpha_1 r_o = 7.35 \times 10^{-3}$ Np. Varying σ_o in accordance with the range of source levels mentioned above, we computed ψ^o_n at particular distances from the source selected for the experiment,[27] giving the axial pressure functions for the fundamental frequency component depicted in Figure 1. It can be seen that our results are in excellent agreement with

measurements except at ranges close to the source (i.e. 0.76 yd and 1.8 yd) where an examination of Figure 6 in Shooter, Muir and Blackstock's article[27] shows that the experimental curves at these distances are not consistently scaled (as they are at all other ranges) to give an extrapolated peak source level at 1 metre. For comparison, computed values of the fundamental, and second harmonic are shown in Figures 2a 2b, and in Figure 3 the "extra decibel loss" is given as a function of R at different source levels corresponding to those of the experiment. Although the harmonic directivity functions for this example are not shown here, they can be computed via Equations (21) and (24) from the data already obtained. Our results have clearly shown however, that the axial field is accurately represented by $\psi_n^o(R)$, thus justifying the assumptions made in deriving Equation (21).

Since the real and imaginary parts of Equation (27) are coupled on the left-hand-side by terms whose coefficient $(1/1 + R^2)$ approaches zero as $1/R^2$ for $R >> 1$, and since the coefficient $\left(1/1 + \dfrac{2m/N}{1 + R^2}\right)$ on the right-hand-side approaches 1 as R increases indefinitely, we now propose to neglect these terms so that recombining the real and imaginary parts of ψ_n^o we obtain an approximate form of Equation (25) given by,

$$\frac{d\psi_n^o}{dR} + \left(\alpha_n r_o + \frac{R}{1 + R^2}\right)\psi_n^o = i\left(\frac{n}{N}\right)\left(\frac{\sigma_o}{4}\right)\left\{\sum_{m=1}^{n-1} \psi_{n-m}^o \psi_m^o + 2\sum_{m=1}^{\infty} \psi_{n+m}^o \psi_m^o\right\} . \quad (28)$$

In this equation the effect of diffraction on the acoustic field is maintained by the spreading-loss term, whose coefficient $(R/1 + R^2)$ approaches zero as R approaches zero and decreases as $1/R$ for $R >> 1$. Using Equation (28) to rederive the unsaturated solution for the second harmonic formed in an inviscid fluid, and comparing it with Rudenko, Soluyan, and Khokhlov's[23] solution of the inviscid form of Equation (25), as given by Equation (A) of Appendix A, we find that neglecting phase differences, the absolute value of the ratio of the two solutions, designated Q, can be expressed as,

$$Q = \frac{\frac{1}{2}\sqrt{\{\mathrm{Ln}(1 + R^2)\}^2 + 4\{\tan^{-1} R\}^2}}{\sinh^{-1} R} \quad . \tag{29}$$

Evaluating the ratio Q as a function of R, it can be seen from Table I that the solution of Equation (28) for the second harmonic, approaches but never exceeds 10% of that derived from Equation (25). It can also be seen from Table I or from inspection of Equation (29) that the difference between the two solutions tends to zero as R approaches zero or infinity. It seems reasonable to assume therefore, that Equation (28) will provide a good approximation to the absolute value of ψ_n^o. Further confirmation of this conclusion is provided by Figures 1 and 2 for the case of Shooter, Muir, and Blackstock's experiment,[27] where values of the fundamental, and second, harmonics computed from Equation (28) are seen to be in good agreement with the results obtained from Equation (25) based on the same numerical procedure.[29]

Using an approach previously adopted by the author[30] in applying Merklinger's[31] heuristic plane wave analysis to the spherical wave form of Burgers' equation, it can be shown that the fundamental frequency component of Equation (28) for a monofrequency source (i.e. $N = 1$) may be represented by means of an approximate expression which differs slightly from a similar approximation obtained heuristically by Merklinger, Mellen, and Moffett.[32] This approximation is given by,

$$\psi_1^o(R) = \frac{e^{-(\alpha_1 r_o)R} \Big/ \sqrt{1 + R^2}}{\sqrt{1 + \left\{\left(\frac{\sigma_o}{2}\right)\int_o^R \frac{e^{-(2\alpha_1 r_o)R'}}{\sqrt{1 + R'^2}}\, dR'\right\}^2}} \tag{30a}$$

$$\rightarrow \frac{e^{-(\alpha_1 r_o)R} \Big/ \sqrt{1 + R^2}}{\sqrt{1 + \left[\frac{\pi\sigma_o}{4}\right]^2 [H_o(2\,\alpha_1 r_o) - Y_o(2\,\alpha_1 r_o)]^2}} \text{, for } R >> 1 \tag{30b}$$

TABLE 1

R	$\frac{1}{2}\sqrt{\{\mathrm{Ln}(1+R^2)\}^2 + 4\{\tan^{-1}R\}^2}$	$\sinh^{-1}R$	Q
10^{-3}	10^{-3}	10^{-3}	1
10^{-2}	10^{-2}	10^{-2}	1
10^{-1}	10^{-1}	10^{-1}	1
1	0.86	0.88	0.98
10	2.74	3.00	0.91
10^2	4.86	5.30	0.92
10^3	7.08	7.60	0.93
10^4	9.34	9.90	0.94

where H_o and Y_o are zero order Struve and Neumann functions, respectively.[33]

As shown in Figure 1, results obtained from Equation (30a) are also in good agreement with those computed directly from Equation (28), thus lending credibility to the approximation.

Another interesting result inherent in the form of Equation (30) is that the finite amplitude absorption loss incurred by the fundamental in propagating through the medium, designated the "extra decibel loss" by Blackstock[34] and hence denoted EXDB , can be expressed as,

$$\begin{aligned} \mathrm{EXDB} &= -20\,\mathrm{Log}_{10}\left|\left(\sqrt{1+R^2}\right)\left(\exp[(\alpha_1 r_o)R]\right)\psi_1^o\right| \\ &= 10\,\mathrm{Log}_{10}\left[1+\left\{\frac{\sigma_o}{2}\int_o^R \frac{e^{-2(\alpha_1 r_o)R'}}{\sqrt{1+R'^2}}\,dR'\right\}^2\right] \qquad (31a) \\ &\rightarrow 10\,\mathrm{Log}_{10}\left\{1+(\pi\sigma_o/4)^2[H_o(2\,\alpha_1 r_o)-Y_o(2\,\alpha_1 r_o)]^2\right\}\ , \\ &\qquad \text{for}\quad R \gg 1\ . \qquad (31b) \end{aligned}$$

Denoting the "extra decibel loss" defined by Equation (31b) as EXDB_∞ to indicate that for fixed values of σ_o it represents the maximum finite-amplitude absorption loss incurred by the fundamental, the curves of Figure 3 were computed showing the variation of this parameter with σ_o and $\alpha_1 r_o$. Since σ_o is related to the source level, as shown in the caption of Figure 4, these characteristics can be used to obtain the "saturation threshold" of a monofrequency source (i.e. the difference between a desired source level and the appropriate value of EXDB_∞) once $\alpha_1 r_o$ and σ_o are specified.

Having provided some degree of justification for Equation (28), we now take its inverse Fourier transform to obtain a new form of Burgers'

equation for a plane piston source, which can be expressed as

$$\frac{\partial\psi}{\partial R} + \left(\frac{R}{1 + R^2}\right)\psi - (\sigma_o/N)\,\psi\,\frac{\partial\psi}{\partial\tau} - (\alpha_o r_o)\,\frac{\partial^2\psi}{\partial\tau^2} = 0 \tag{32}$$

where $$\psi(R,\tau) = \sum_{n=-\infty}^{\infty} \psi_n^o(R)\, e^{in\tau} \quad . \tag{33}$$

It can be seen by inspection that if $R \ll 1$, Equation (32) approaches the plane wave form of Burgers' equation. Alternatively, if $R \gg 1$, it assumes the spherical wave form of Burgers' equation, as required.

Assuming further that the axial field is determined primarily by $\psi_n^o(R)$ it follows from Equation (14) that

$$u(R,o,\tau) \simeq \psi(R,\tau) \quad . \tag{34}$$

In order to obtain the Fubini,[35,36] Fay,[37-40] and asymptotic far field[34,41] solutions of Equation (32), it is convenient to reexpress it in terms of the 'stretched coordinate' system introduced by Blackstock.[24] This transformation is carried out in Appendix B yielding the scaled form of Equation (32) prescribed by Equation (B7) as,

$$\frac{\partial W}{\partial\sigma} - (1/N)\,W\,\frac{\partial W}{\partial\tau} - \left\{\Gamma_o^{-1}\cosh(\sigma/\sigma_o)\right\}\frac{\partial^2 W}{\partial\tau^2} = 0 \tag{35}$$

where $$W = \psi\sqrt{1 + R^2} \tag{36}$$

and $$\sigma/\sigma_o = F(R) = \sinh^{-1} R \quad . \tag{37}$$

The established solutions[35-41] of Equation (32) for a monofrequency source are outlined in Appendix B, but before concluding it should be noted that

the unspecified "distortion function" $F(R)$ previously mentioned in the text has now been equated to $\sinh^{-1} R$ in Equation (37). Strictly speaking, a more precise form of $F(R)$ for the case of Equation (21) would be the numerator of Equation (29), but as we have shown in Table I, this differs only marginally from $\sinh^{-1} R$.

Having thus completed our discussion of the field equations governing the propagation of finite-amplitude waves radiated by a plane piston projector, we will now consider how these equations can be used to provide scaling laws for parametric receiving arrays.

2. Parametric Receiving Arrays

Since the analytical model that has been developed can be used to define the field of a finite-amplitude pump wave radiated by a plane piston projector under saturated or unsaturated conditions, we now wish to consider the up-converted fields generated via interaction between the pump and a plane wave of angular frequency Ω whose wave normal intersects the pump axis (i.e. the positive z axis) at an angle Θ. We begin by expressing the component of the signal along the pump axis in the form,

$$\begin{aligned} u_s(z,t) &= \mathrm{Re}\left\{ u_{s_o} e^{i(\Omega t - X_\Omega z \cos\Theta)} \right\} \\ &= \mathrm{Re}\left\{ u_{s_o} e^{i(\Omega t - X_\Omega z + 2M_\Omega z} \right\} \\ &= \mathrm{Re}\left\{ u_{s_o} e^{-\alpha_\Omega z + i(\Omega t - k_\Omega z + 2M_\Omega z)} \right\} \end{aligned} \tag{38}$$

where $X_\Omega = k_\Omega - i\alpha_\Omega$, and $M_\Omega = X_\Omega \sin^2(\Theta/2)$. (39)

We now let $\tau = \Omega(t - z/c_o) = (\Omega t - k_\Omega z)$, $R = z/r_o$, and $r_o = k_o a^2/2$ so that Equation (38) becomes,

$$u_s(R,\tau) = \mathrm{Re}\left\{ u_{s_o} e^{-(\alpha_\Omega r_o)R + i[\tau + (2M_\Omega r_o)R]} \right\} . \tag{40}$$

If ω_o is the pump frequency, we arbitrarily chose its time waveform at the source to be,

$$u_p(o,\tau) = \sin(N\tau) \quad ; \qquad N = \omega_o/\Omega . \tag{41}$$

The spectral amplitude of the component of the signal along the pump axis can thus be expressed as

$$\psi_1^o(R) = \psi_s^o(R)$$

$$= \psi_{s_o}^o e^{-(\alpha_1 r_o)R + i(2M_\Omega r_o)R} \; ; \qquad \psi_{s_o} = u_{s_o} \, , \, \alpha_1 = \alpha_\Omega \quad (42)$$

hence from Equation (26) we have,

$$\overline{\psi_1^o}(R) = \psi_{s_o}^o e^{-(\alpha_1 r_o)R} \cos(2M_\Omega r_o R) \quad (43a)$$

$$\hat{\psi}_1^o(R) = -\psi_{s_o}^o e^{-(\alpha_1 r_o)R} \sin(2M_\Omega r_o R) \; . \quad (43b)$$

Likewise, the spectral amplitudes of the pump wave at the source can be arbitrarily expressed as,

$$\psi_N^o(0) = \psi_p^o(0) \quad (44)$$

giving $\overline{\psi_N^o}(0) = 0$ (45a)

and $\hat{\psi}_N^o(0) = 1$. (45b)

With the boundary conditions for the pump field prescribed by Equations (45a) and (45b), we can now solve Equation (27) numerically to determine the up-converted frequency components $\psi_{N\pm1}^o(R)$ using Equations (43a) and (43b) to define $\overline{\psi_1^o}(R)$ and $\hat{\psi}_1^o(R)$ throughout the field. This calculation can be repeated using different values of N , $(\alpha_N r_o)$, and σ_o in order to express the 'signal excess' $\psi_{N\pm1}^o/\psi_{s_o}^o$ as a function of the pump amplitude via the parameter σ_o for particular values of $(\alpha_N r_o)$ and R . These calculations

must then be repeated for different values of Θ in order to determine the spatial directivities of the up-converted fields. Since this is a very lengthy process it is expedient to take advantage of the fact that in most applications of interest the signal is considered to be very weak relative to the pump. The equations for the up-converted spectral amplitudes $\psi^o_{\underline{N+1}}$ can thus be considerably simplified by neglecting terms on the right-hand-side of Equation (25) other than those that involve direct products of the pump and signal components giving,

$$\frac{d\psi^o_{N+1}}{dR} + \left(\alpha_{N+1}r_o - \frac{i}{1-iR}\right)\psi^o_{N+1} = i\left(\frac{N+1}{N}\right)\left(\frac{\sigma_o}{4}\right)\left\{\sum_{m=1}^{N}\psi^o_{N+1-m}\psi^o_m + 2\sum_{m=1}^{\infty}\psi^o_{n+1+m}\psi^{o*}_m\right\}$$

$$\simeq i\left(\frac{N+1}{N}\right)\left(\frac{\sigma_o}{4}\right)\sum_{m=1}^{N}\psi^o_{N+1-m}\psi^o_m$$

$$= i\left(\frac{N+1}{N}\right)\left(\frac{\sigma_o}{2}\right)\psi^o_N\psi^o_1 \qquad (46a)$$

$$\frac{d\psi^o_{N-1}}{dR} + \left(\alpha_{N-1}r_o - \frac{i}{1-iR}\right)\psi^o_{N-1} = i\left(\frac{N-1}{N}\right)\left(\frac{\sigma_o}{4}\right)\left\{\sum_{m=1}^{N-2}\psi^o_{N-1-m}\psi^o_m + 2\sum_{m=1}^{\infty}\left[\frac{1}{1+\frac{2m/N}{1+R^2}}\right]\psi^o_{N-1+m}\psi^{o*}_m\right\}$$

$$\simeq i\left(\frac{N-1}{N}\right)\left(\frac{\sigma_o}{2}\right)\sum_{m=1}^{\infty}\left[\frac{1}{1+\frac{2m/N}{1+R^2}}\right]\psi^o_{N-1+m}\psi^{o*}_m$$

$$= i\left(\frac{N-1}{N}\right)\left(\frac{\sigma_o}{2}\right)\sum_{m=1}^{\infty}\left\{\left[\frac{1}{1+\frac{2/N}{1+R^2}}\right]\psi^o_N + \left[\frac{1}{1+\frac{2}{1+R^2}}\right]\psi^{o*}_N\right\}\psi^{o*}_1 \, . \qquad (46b)$$

Under unsaturated conditions the pump field is given approximately by Equation (25) as

$$\psi^o_N(R) = \frac{e^{-(\alpha_N r_o)R}}{1-iR} \, . \qquad (47)$$

Substituting Equations (42) and (47) in the right-hand-side of Equation (46a) we thus obtain,

$$\frac{d\psi^o_{N+1}}{dR} + \left(\alpha_{N+1}r_o - \frac{i}{1 - iR}\right)\psi^o_{N+1} = i\left(\frac{N+1}{N}\right)\left(\frac{\sigma_o}{2}\right)\psi^o_{s_o}\,\frac{e^{-(\alpha_N r_o + \alpha_1 r_o)R + i(2M_\Omega r_o)R}}{1 - iR}\,. \tag{48}$$

Since $\psi^o_{N+1}(0) = 0$, the solution of Equation (48) enables the 'signal excess' $\psi^o_{N+1}/\psi^o_{s_o}$ for the upper sideband to be expressed as,

$$\psi^o_{N+1}/\psi^o_s = i\left(\frac{N+1}{N}\right)\left(\frac{\sigma_o}{2}\right)\frac{e^{-(\alpha_{N+1}r_o)R}}{1 - iR}\int_o^R e^{i(2M_\Omega r_o)R'}\,dR'$$

$$= i\left(\frac{N+1}{N}\right)\left(\frac{\sigma_o}{2}\right)\frac{R}{\sqrt{1+R^2}}\left(\frac{\sin\{(M_\Omega r_o)R\}}{(M_\Omega r_o)R}\right)e^{-(\alpha_{N+1}r_o)R + i\{\tan^{-1}R + (M_\Omega r_o)R\}}. \tag{49}$$

By means of the plane wave impedance relationship, we can reexpress the signal excess as $\psi^o_{N+1}/\psi^o_{s_o} = p'_+/p'_{s_o}$ so that in terms of more conventional notation Equation (49) becomes,

$$p'_+/p'_{s_o} = i\left(\frac{\omega_+}{\omega_o}\right)\left(\frac{\sigma_o}{2}\right)\frac{R}{\sqrt{1+R^2}}\left(\frac{\sin\{(X_\Omega r_o)R\sin^2(\Theta/2)\}}{(X_\Omega r_o)R\sin^2(\Theta/2)}\right)e^{-(\alpha_+ r_o)R + i\{\tan^{-1}R + (X_\Omega r_o)R\sin^2(\Theta/2)\}}. \tag{50}$$

Inspection of Equation (50) shows that if $R \ll 1$ it approaches Berktay and Al.Temimi's solution[10] for a plane pump wave, and likewise if $R \gg 1$ it approaches the form of the corresponding spherical pump wave solution, utilized by Goldsberry[17] and McDonough[18] in their respective systems studies. Since Equation (50) is perfectly general and can easily be incorporated in such studies it should prove useful in cases where the pump projector Rayleigh distance is large.

Returning now to Equation (46b) and substituting Equations (42) and (47) in the right hand side we obtain,

$$\frac{d\psi^o_{N-1}}{dR} + \left(\alpha_{N-1}r_o - \frac{i}{1 - iR}\right)\psi^o_{N-1} = i\left(\frac{N-1}{N}\right)\left(\frac{\sigma_o}{2}\right)\psi^o_{s_o}\left\{\left(\frac{1/1 - iR}{1 + \frac{2/N}{1+R^2}}\right) + \left(\frac{1/1 + iR}{1 + \frac{2}{1+R^2}}\right)\right\}$$

$$e^{-(\alpha_N r_o + \alpha_1 r_o)R - i(2M_\Omega r_o)R}$$

$$\simeq i\left(\frac{N-1}{N}\right)\left(\frac{\sigma_o}{2}\right)\psi^o_{s_o}\left\{1 + \left(\frac{1 - iR}{1 + iR}\right)\left(\frac{1 + R^2}{3 + R^2}\right)\right\}$$

$$\frac{e^{-(\alpha_N r_o + \alpha_1 r_o)R - i(2M_\Omega r_o)R}}{1 - iR}$$

$$\approx i\left(\frac{N-1}{N}\right)\left(\frac{2\sigma_o}{3}\right)\psi^o_{s_o}\frac{e^{-(\alpha_N r_o + \alpha_1 r_o)R - i(2M_\Omega r_o)R}}{1 - iR}. \tag{51}$$

Hence with $\psi^o_{N-1}/\psi^o_{s_o} = p'_-/p'_{s_o}$ the solution of Equation (51) gives,

$$p'_-/p'_{s_o} = i\left(\frac{\omega_-}{\omega_o}\right)\left(\frac{2\sigma_o}{3}\right)\frac{R}{\sqrt{1 + R^2}}\left\{\frac{\sin\,(X_\Omega r_o)R\,\sin^2(\Theta/2)}{(X_\Omega r_o)R\,\sin^2(\Theta/2)}\right\}e^{-(\alpha_- r_o)R + i\{\tan^{-1}R - (X_\Omega r_o)R\,\sin^2(\Theta/2)\}}. \tag{52}$$

Comparison of Equations (50) and (52) shows that with the exception of a slight change of phase the two solutions agree to within a factor $\frac{4}{3}\left(\frac{\omega_-}{\omega_+}\right)e^{-(\alpha_- r_o - \alpha_+ r_o)R}$ $\simeq \frac{4}{3}\left(\frac{\omega_-}{\omega_+}\right) \simeq 1$.

Since we are primarily concerned with the effect of a saturated pump field upon the up-converted frequency components we now repeat the previous derivation of $\psi^o_{N\pm1}$ using Equation (30a) in place of Equation (47) to define

the pump field. In this manner, neglecting the small difference between ψ_+^o and ψ_-^o, the signal excess $p'_\pm/p'_{s_o}$ can be expressed as,

$$p'_\pm/p'_{s_o} = i\left(\frac{\omega_\pm}{\omega_o}\right)\left(\frac{\sigma_o}{2}\right)\frac{e^{-(\alpha_\pm r_o)R + i\tan^{-1}R}}{\sqrt{1+R^2}}\int_o^R \frac{e^{i(2M_\Omega r_o)R'}\,dR'}{\sqrt{1+\left(\frac{\sigma_o}{2}\int_o^{R'}\frac{e^{-(2\alpha_N r_o)R''}}{\sqrt{1+R''^2}}\,dR''\right)^2}}$$

$$= i\left(\frac{\omega_\pm}{\omega_o}\right)\left(\frac{\sigma_o}{2}\right)\frac{e^{-(\alpha_\pm r_o)R + i\tan^{-1}R}}{\sqrt{1+R^2}}\sum_{m=-\infty}^{\infty}\exp\{i\,m\,\sin^{-1}(\sin^2\Theta/2)\}\int_o^R$$

$$\frac{J_m(2X_\Omega r_o R')\,dR'}{\sqrt{1+\left(\frac{\sigma_o}{2}\int_o^{R'}\frac{e^{-(2\alpha_N r_o)R''}}{\sqrt{1+R''^2}}\,dR''\right)^2}} \qquad (53)$$

On axis this becomes,

$$p'_\pm/p'_{s_o}\underset{\Theta=0}{\to} i\left(\frac{\omega_\pm}{\omega_o}\right)\left(\frac{\sigma_o}{2}\right)\frac{e^{-(\alpha_\pm r_o)R + i\tan^{-1}R}}{\sqrt{1+R^2}}\int_o^R \frac{dR'}{\sqrt{1+\left(\frac{\sigma_o}{2}\int_o^{R}\frac{e^{-(2\alpha_N r_o)R''}}{\sqrt{1+R''^2}}\,dR''\right)^2}} \qquad (54)$$

Likewise, if $D_\pm(\Theta)$ denotes the spatial directivity functions of the up-converted fields then from Equation (53),

$$D_\pm(\Theta) = \frac{\displaystyle\sum_{m=-\infty}^{\infty}\exp\{i\,m\,\sin^{-1}(\sin^2\Theta/2)\}\int_o^R\frac{J_m(2X_\Omega r_o R')\,dR'}{\sqrt{1+\left(\frac{\sigma_o}{2}\int_o^{R'}\frac{e^{-(2\alpha_N r_o)R''}}{\sqrt{1+R''^2}}\,dR''\right)^2}}}{\displaystyle\int_o^R\frac{dR'}{\sqrt{1+\left(\frac{\sigma_o}{2}\int_o^{R}\frac{e^{-(2\alpha_N r_o)R''}}{\sqrt{1+R''^2}}\,dR''\right)^2}}} \quad . \qquad (55)$$

Evaluating Equations (54) and (55) numerically we obtained the results depicted in Figures 5a and 5b which clearly show in terms of 'scaled' coordinates the effect of pump wave saturation upon the up-conversion process.

Finally, in order to obtain simple numerical estimates for values of $\alpha_N r_o \equiv \alpha_o r_o < 0.1$, we make use of weak shock theory by substituting $\psi_N^o(R) \simeq e^{-(\alpha_N r_o)R} / [1 + \frac{\sigma_o}{2} \mathrm{Ln}(1 - iR)]$ in Equations (46a) and (46b) to obtain,

$$p'_{\pm}/p'_{s_o} = -\left(\frac{\omega_{\pm}}{\omega_o}\right)\left\{ \mathrm{Ei}\left[\frac{2}{\sigma_o}\left(1 - i\frac{\sigma_o}{2}R\right)\right] - \mathrm{Ei}\left[\frac{2}{\sigma_o}\right]\right\} \frac{e^{-(\alpha_{\pm} r_o)R + i\tan^{-1}R - 2/\sigma_o}}{\sqrt{1+R^2}} \tag{56}$$

$$\simeq -\left(\frac{\omega_{\pm}}{\omega_o}\right) \frac{\mathrm{Ln}\,[1 - i\frac{\sigma_o}{2}R]}{\sqrt{1+R^2}} e^{-(\alpha_{\pm} r_o)R + i\tan^{-1}R}\,, \quad \sigma_o > 1 \tag{57a}$$

$$\rightarrow i\left(\frac{\omega_{\pm}}{\omega_o}\right)\left(\frac{\sigma_o}{2}\right) \frac{R}{\sqrt{1+R^2}} e^{-(\alpha_{\pm} r_o)R + i\tan^{-1}R}\,, \quad \sigma_o R/2 < 1 \tag{57b}$$

$$\rightarrow -\left(\frac{\omega_{\pm}}{\omega_o}\right) \frac{1}{2}\sqrt{\frac{\left\{\mathrm{Ln}\left|1 + \left(\frac{\sigma_o}{2}R\right)^2\right|\right\}^2 + 4\left\{\tan^{-1}\left(\frac{\sigma_o R}{2}\right)\right\}^2}{1+R^2}}\; e^{-(\alpha_{\pm} r_o)R + i\tan^{-1}R}\,, \quad \sigma_o R/2 > 1 \tag{57c}$$

Having thus obtained approximate expressions for the signal excess, the "pump excess" p'_1/p'_+ can likewise be approximated by means of Equations (3_a) and (50) or (57c).

Since the "signal excess" as defined by Equation (57c) is virtually independent of $\omega_{\pm}/\omega_o$ for $\omega_o >> \Omega_s$ it follows that "scaled characteristics" giving the functional dependence of $\left|(p'_{\pm}/p'_{s_o}) \exp\{(\alpha_{\pm} r_o)R\}\right|$ on σ_o can readily be constructed for different values of the "scaled range" R , as shown in Figure 6, where the particular choice of R equal to 10 and 100 respectively, was quite arbitrary. Using such characteristics, the signal

excess can readily be evaluated. For example, in the case of a 100 kHz pump wave radiated by a 0.3m diameter projector in fresh water, with $r_o = 4.7m$, $\alpha_1 = 2.6 \times 10^{-4}$ Np/m , and $\alpha_1 r_o = 1.23 \times 10^{-3}$ Np , Figure 6 gives the signal excess measured by a hydrophone located on the pump axis at $R = 100$ (i.e. $r = 470m$) for $0.01 \leq \sigma_o \leq 1$ as,

σ_o	Radiated Pump Power Watts	Signal Excess dB
0.01	2×10^{-3}	-67
0.1	2×10^{-1}	-53
1.0	2×10^{3}	-47

It is clear from this example therefore, that increasing the radiated pump power to enhance the signal excess reaches a point of diminishing returns when $\sigma_o = 1$; a conclusion which is further confirmed by examining the degradation of the directivity functions as σ_o increases.

Conclusions

Using Kuznetsov's[20] nonlinear paraxial wave equation to derive coupled spectral equations for the axial field of a finite-amplitude pump wave radiated by a plane piston projector, we have shown both by numerical analysis and by successive approximation that the solutions of these equations are in good agreement with well established experimental results[27] under saturated and unsaturated conditions. We have also shown that when the pump field is modulated by the spatial component of a weak field transmitted along the pump axis that the resulting up-converted frequency components can be amplified by increasing the amplitude of the pump wave until a point of diminishing returns is reached when the latter exceeds its saturation threshold. In order to supplement our numerical analysis of the up-conversion process, we have derived analytical expressions for the signal excess and pump excess which are in reasonably good agreement with our numerical results for values of the small-signal-pump-wave-absorption-loss $\alpha_o r_o$ less than 0.1 np. These closed form approximations, which reduce at low pump amplitudes to Berktay and Al. Temimi's[10] spherical pump wave solution, are sufficiently simple to be readily included in system simulation models where they can define upper bounds for the conversion efficiency and directivity of Parametric Receiving Arrays as the pump wave undergoes saturation.

Acknowledgement

This work was supported by ARPA under contract N00039-75-C-0259.

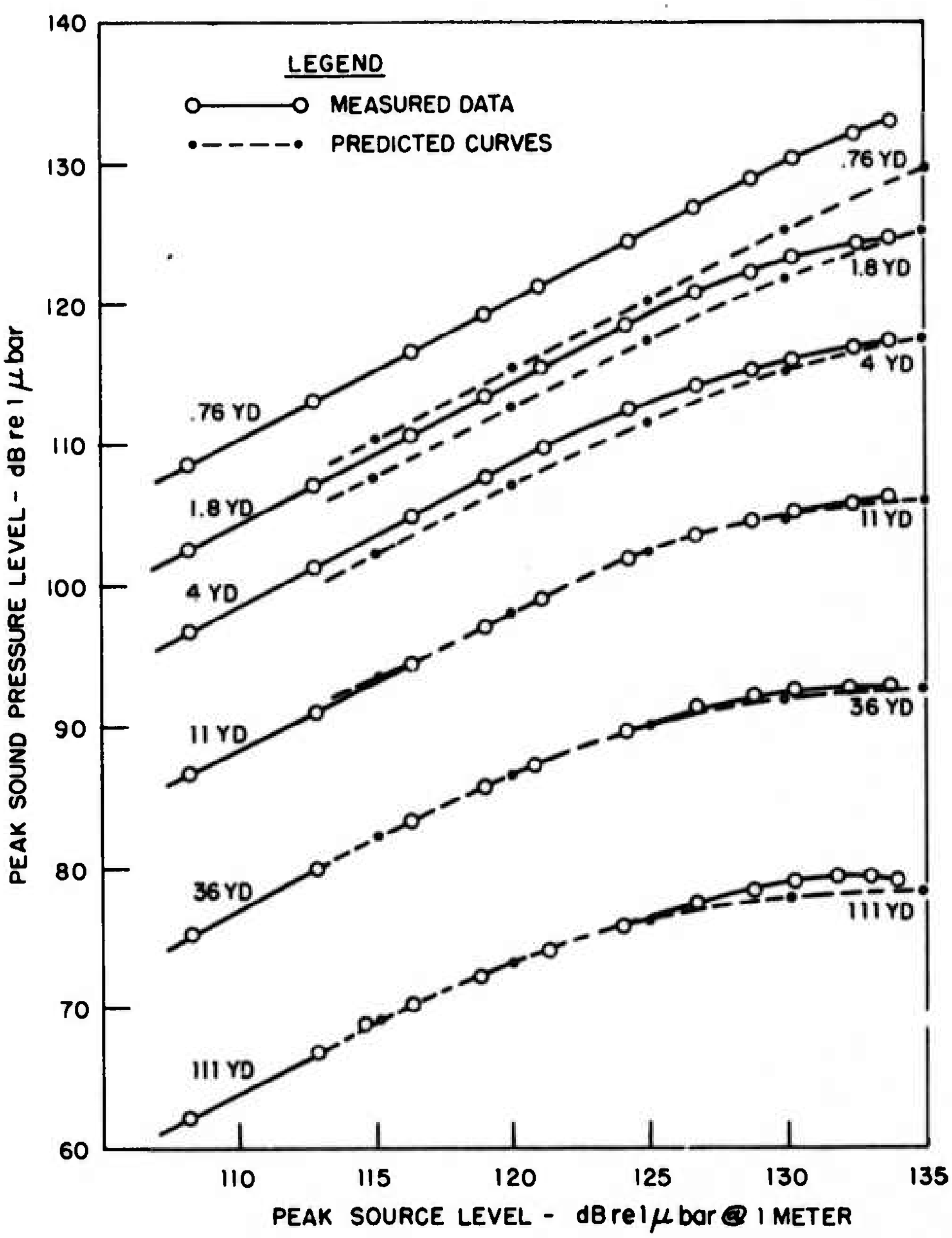

Figure 1. Axial Pressure Field of a 454 kHz Signal Radiated by a 3" Diameter Projector in Fresh Water [r_o = 1.5 yds, $\alpha_1 r_o = 7.35 \times 10^{-3}$ Np, B/A = 4.9].

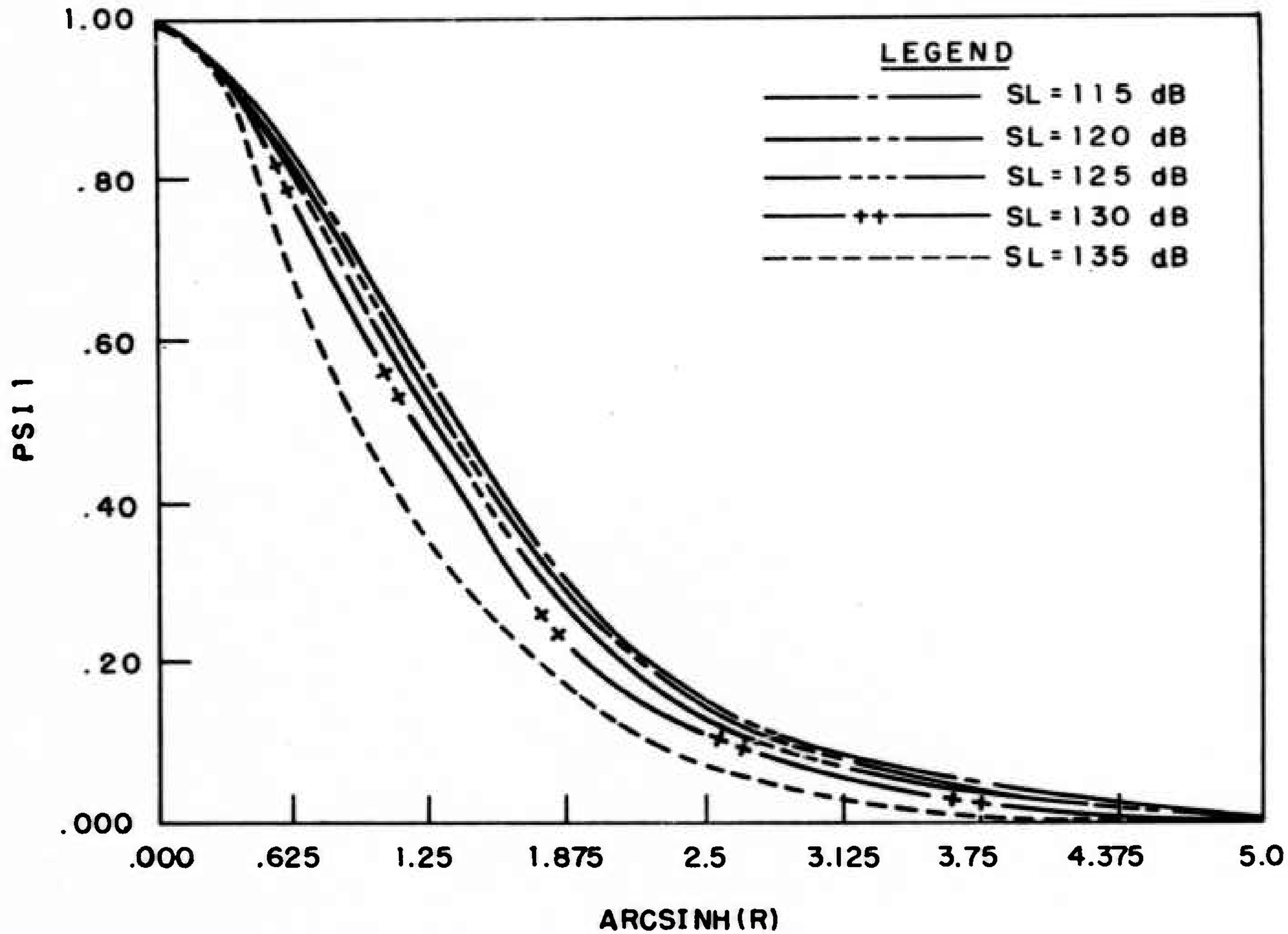

Figure 2a. Axial Pressure Field of a 454 kHz Signal in Fresh Water.

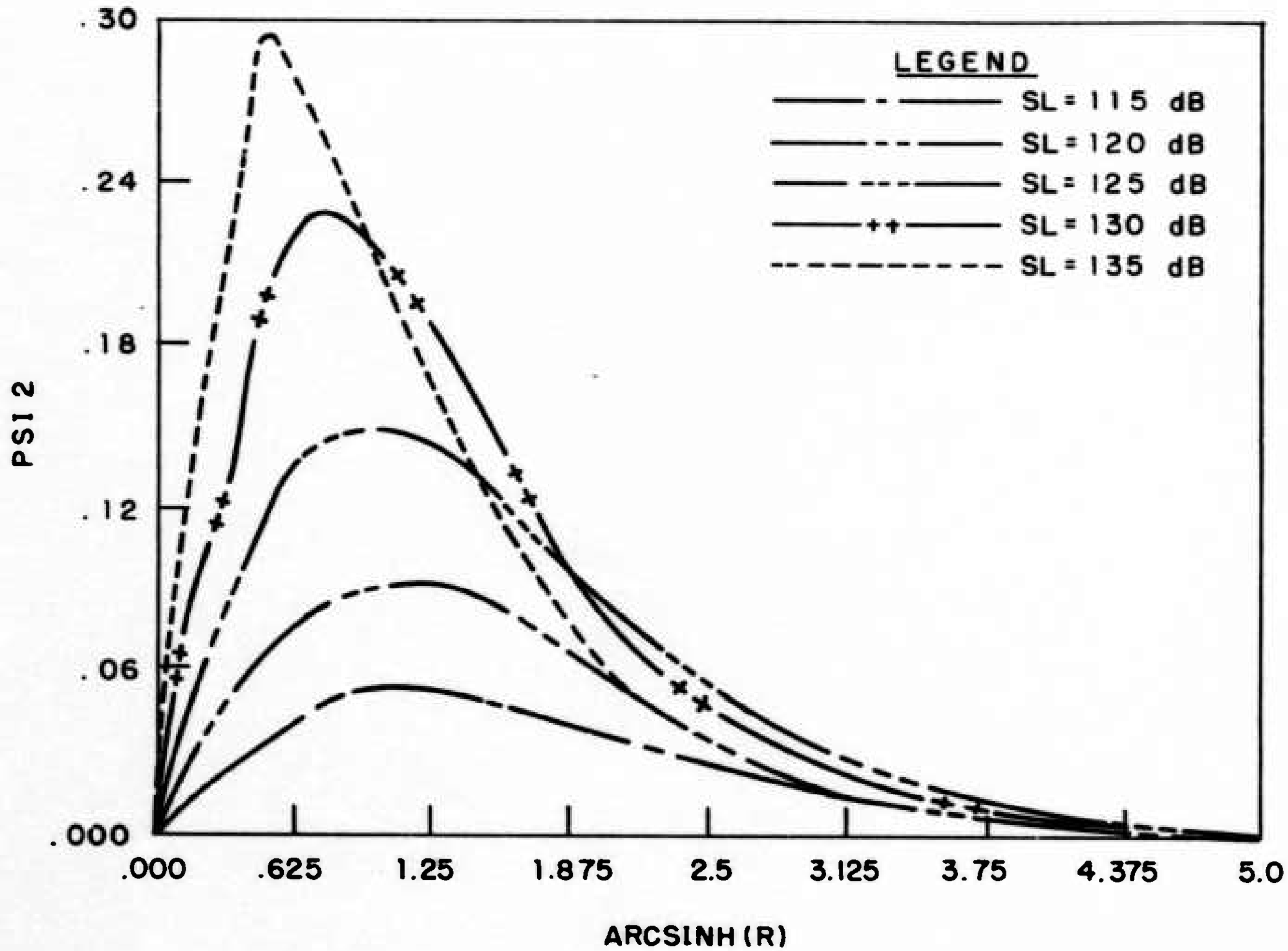

Figure 2b. Axial Pressure Field for the Second Harmonic of a 454 kHz Signal Generated Via Nonlinear Self-Interaction of the Fundamental in Fresh Water.

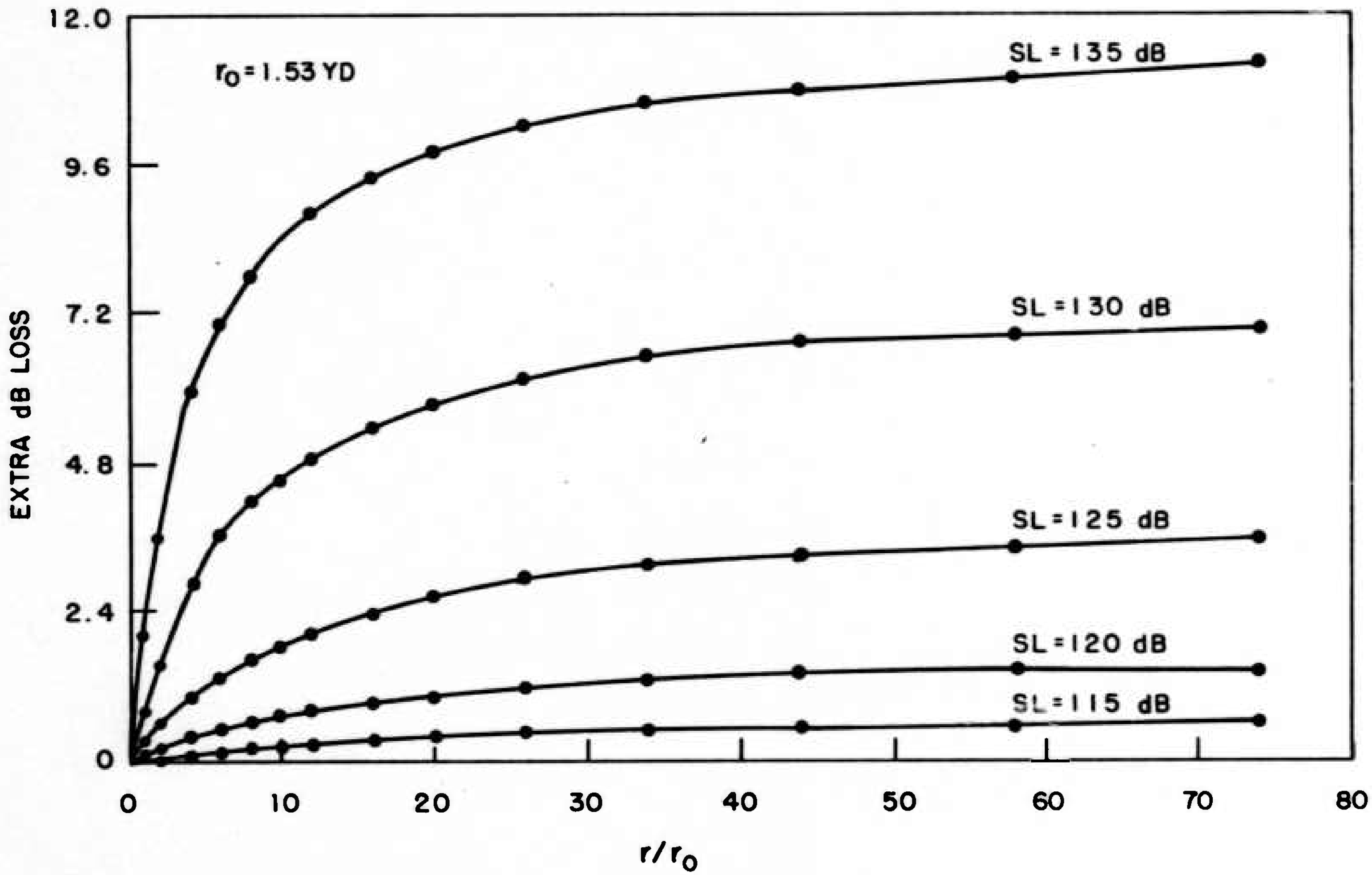

Figure 3. Finite-Amplitude Absorption Losses Incurred by a 454 kHz Signal in Fresh Water.

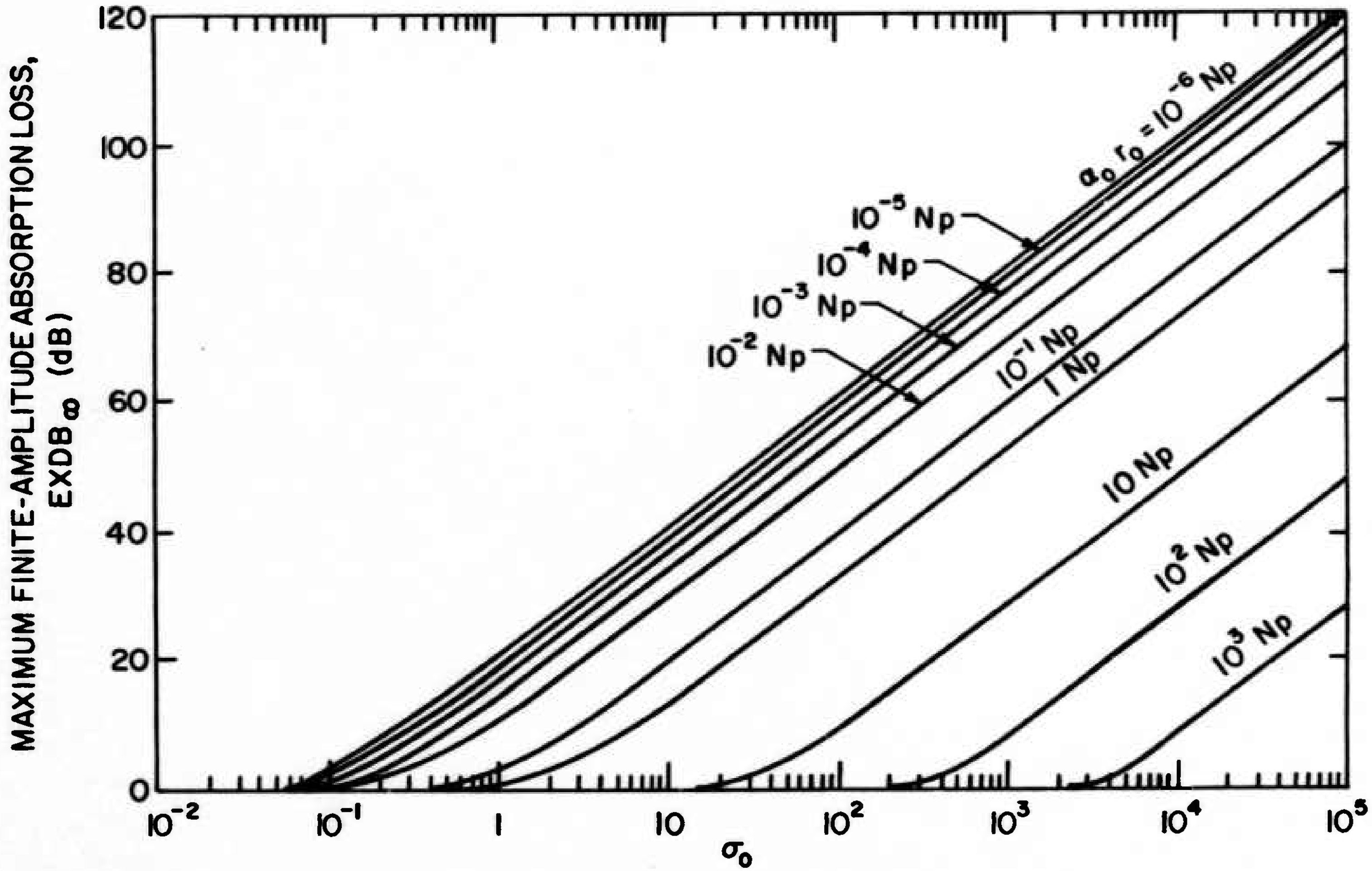

Figure 4. Far-Field Finite-Amplitude Absorption Characteristics

$[20 \log_{10}\sigma_o = SL_o + 20 \log_{10} (\sqrt{2}\beta k_o/\rho_o c_o^2) \equiv SL_o^* + 20 \log_{10} (2\pi \sqrt{2}\beta \times 10^{-3}/\rho_o c_o^3)$

$= SL_o^* - 180$ dB in water (1 μbar = reference pressure)

where $SL_o = 20 \log(p_o r_o/\sqrt{2})$ and $SL_o^* = 20 \log (p_o r_o f_o/\sqrt{2})$; f_o in kHz].

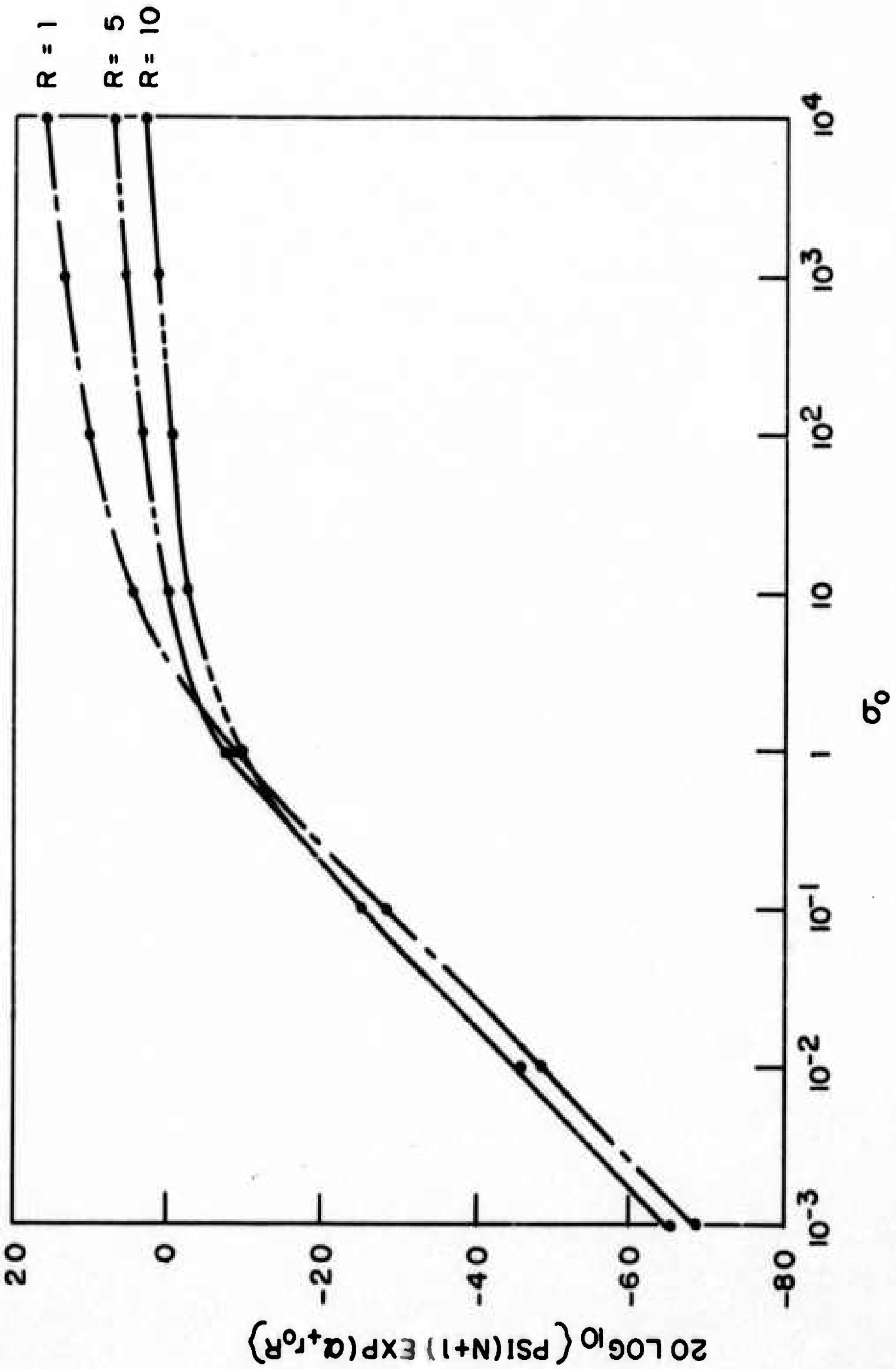

Figure 5a. Signal-Excess Characteristics

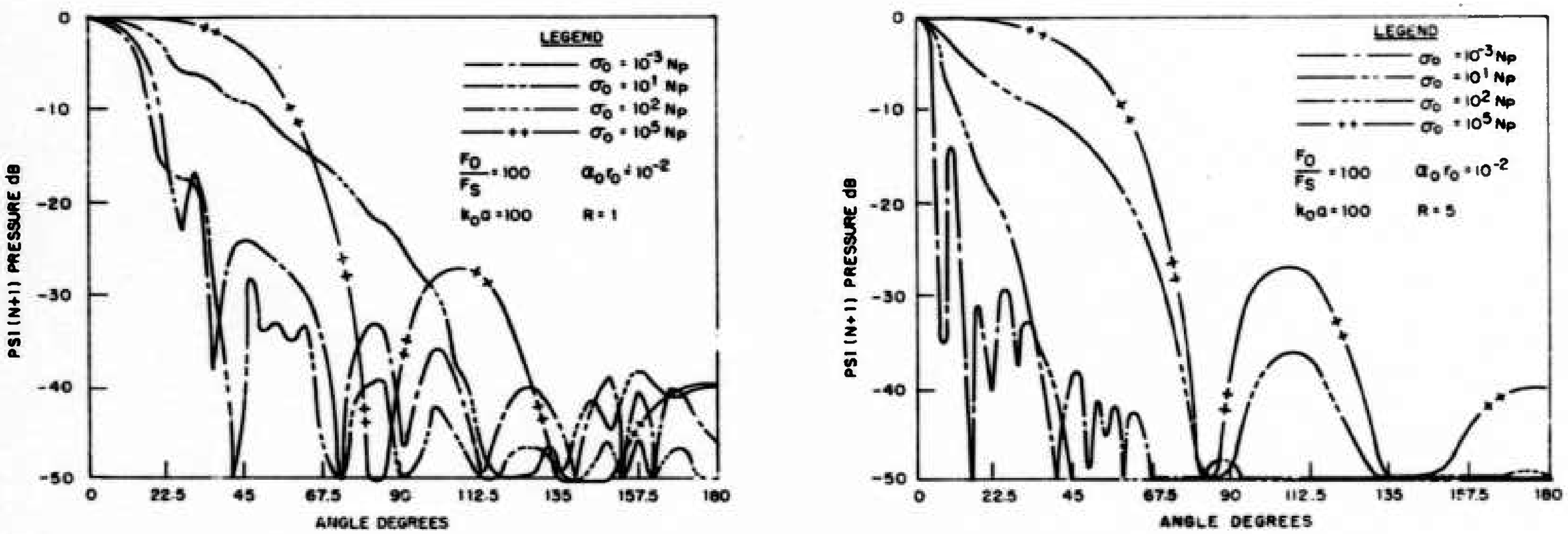

Figure 5b. Up-Converted Directivity Characteristics

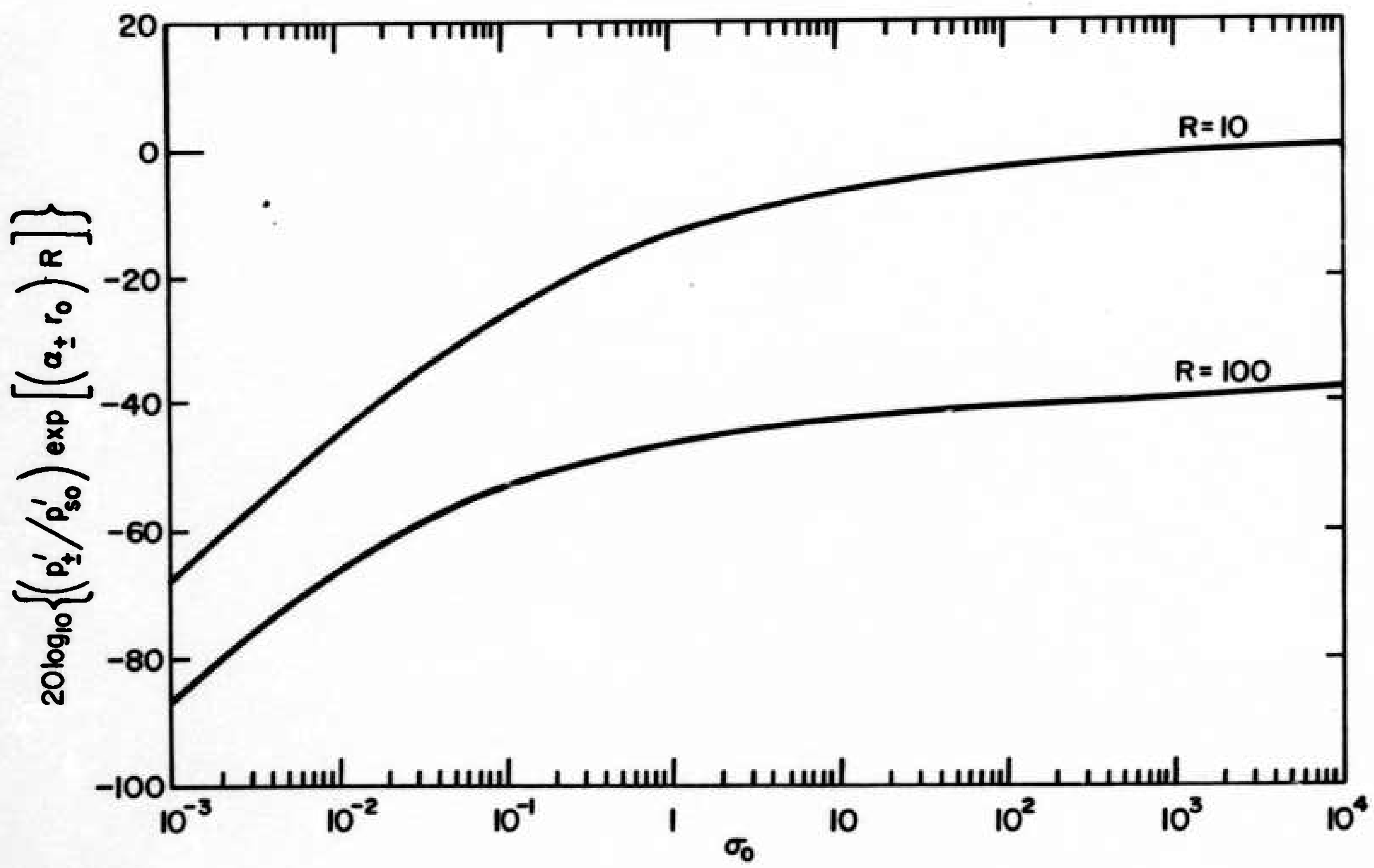

Figure 6. Approximate Signal-Excess Characteristics

APPENDIX A

For an unsaturated monofrequency source of finite-amplitude (i.e. $\sigma_o < 1$, $N = 1$) the spectral amplitude of the fundamental frequency component is obtained throughout the field, to a first approximation, by suppressing the right-hand-side of Equation (22) so that,

$$\frac{d\psi_1^o}{dR} + \left(\alpha_1 r_o - \frac{i}{1 - iR}\right)\psi_1^o = 0 \quad , \quad \psi_1^o(0) = 1 \tag{A1}$$

giving
$$\psi_1^o(R) = \frac{e^{-(\alpha_1 r_o)R}}{1 - iR} \quad . \tag{A2}$$

Substituting Equation (A2) in the right-hand-side of Equation (22), the spectral amplitude of the second harmonic field generated by self-interaction of the fundamental frequency component in the medium is given to second-order by the equation,

$$\frac{d\psi_2^o}{dR} + \left(\alpha_2 r_o - \frac{i}{1 - iR}\right)\psi_2^o = \frac{i\sigma_o}{2}\,\frac{e^{-2\alpha_1 r_o R}}{[1 - iR]^2} \quad ; \quad \alpha_2 = 4\alpha_1 \tag{A3}$$

hence,

$$\psi_2^o(R) = \frac{i\sigma_o}{2}\,\frac{e^{-(\alpha_2 r_o)R}}{1 - iR}\int_o^R \frac{e^{(\alpha_2 r_o - 2\alpha_1 r_o)R'}}{1 - iR'}\,dR'$$

$$= -\frac{\sigma_o}{2}\,\frac{e^{-(4\alpha_1 r_o)R - i(2\alpha_1 r_o)}}{1 - iR}\int_o^{1 - iR}\frac{e^{i(2\alpha_1 r_o)y}}{y}\,dy$$

$$= -\frac{\sigma_o}{2}\,\frac{e^{-(4\alpha_1 r_o)R - i(2\alpha_1 r_o)}}{1 - iR}\left\{E_i[i(2\alpha_1 r_o)(1 - iR)] - E_i[i(2\alpha_1 r_o)]\right\} \tag{A4}$$

where $$Ei(x) = \int_{-\infty}^{x} \frac{e^{y}}{y}\, dy \quad . \tag{A5}$$

From the asymptotic limits of $Ei(x)$ we obtain, for $\alpha_1 r_o >> 1$,

$$\psi_2^o(R) \rightarrow -\frac{\Gamma_o}{4}\left\{\frac{e^{-(2\alpha_1 r_o)R}}{(1 - iR)^2} - \frac{e^{-(4\alpha_1 r_o)R}}{(1 - iR)}\right\}$$

$$= -\frac{\Gamma_o}{4}\left\{\frac{e^{-(2\alpha_1 r_o)R + 2i\tan^{-1}R}}{(1 + R^2)} - \frac{e^{-(4\alpha_1 r_o)R + i\tan^{-1}R}}{\sqrt{1 + R^2}}\right\} \tag{A6}$$

Alternatively, as $\alpha_1 r_o \rightarrow 0$,

$$\psi_2^o(R) \rightarrow -\frac{\sigma_o}{2}\,\frac{Ln(1 - iR)}{1 - iR}$$

$$= -\frac{\sigma_o}{4}\sqrt{\frac{\{Ln(1 + R^2)\}^2 + 4\,\{\tan^{-1}R\}^2}{1 + R^2}}\; e^{\,i\tan^{-1}R - \tan^{-1}\left\{\frac{2\tan^{-1}R}{Ln(1 + R^2)}\right\}} \tag{A7}$$

This inviscid solution is identical to that obtained by Rudenko, Soluyan, and Khokhlov.[23]

APPENDIX B

Combined Plane-Spherical-Wave Burgers' Equation in Stretched Coordinates

Following Blackstock[24] we chose to redefine ψ in terms of a new variable W, defined as,

$$W = \psi\sqrt{1 + R^2} \quad . \tag{B1}$$

Substituting Equation (B1) in Equation (30), we obtain,

$$\frac{\partial W}{\partial R} - \left[\sigma_o / N\sqrt{1 + R^2}\right] W \frac{\partial W}{\partial \tau} - (\alpha_o r_o) \frac{\partial^2 W}{\partial \tau^2} = 0 \quad . \tag{B2}$$

Again, following Blackstock,[24] we introduce the scaled distortion distance $\sigma = {}_oF(R)$ in Equation (B2), where $F(R)$ has yet to be defined, giving

$$\frac{\partial W}{\partial \sigma} - \left[1/NF'(R)\sqrt{1 + R^2}\right] W \frac{\partial W}{\partial \tau} - [1/\Gamma_o \; F'(R)] \frac{\partial^2 W}{\partial \tau^2} = 0 \quad ;$$

$$\Gamma_o = \sigma_o / \alpha_o r_o \quad . \tag{B3}$$

The function $F(R)$ can now be defined by setting $F'(R) = 1/\sqrt{1 + R^2}$ so that,

$$F(R) = \int_o^R \frac{dR'}{\sqrt{1 + R'^2}}$$

$$= \sinh^{-1} R \tag{B4}$$

hence $\sigma = \sigma_o \sinh^{-1} R$; $R = \sinh(\sigma/\sigma_o)$. (B5)

Frim Equations (B4) and (B5) we thus have

$$F'(R) = \frac{1}{\sqrt{1 + R^2}}$$

$$= \frac{1}{\cosh(\sigma/\sigma_o)} \quad . \qquad \text{(B6)}$$

Finally, substituting Equation (B6) in Equation (B3) the combined plane-spherical wave form of Burgers' equation expressed in terms of 'stretched' coordinates becomes,

$$\frac{\partial W}{\partial \sigma} - (1/N)\, W \frac{\partial W}{\partial \tau} - \left\{ \Gamma_o^{-1} \cosh(\sigma/\sigma_o) \right\} \frac{\partial^2 W}{\partial \tau^2} = 0 \quad . \qquad \text{(B7)}$$

For a monofrequency source (i.e. $N = 1$) the solution of Equation (B7) can be expressed via the Fubini,[35,36] Fay,[37-40] and asymptotic far-field[34,41] approximations as,

$$W(\sigma,\tau) = \sum_{n=1}^{\infty} \frac{2J_n(n\sigma)}{n\sigma} \sin(n\tau) \quad , \qquad o \leq \sigma \leq 1 \quad \text{(B8a)}$$

$$= \frac{2}{\Gamma_o} \sum_{n=1}^{\infty} \frac{\cosh(\sigma/\sigma_o)\sin(n\tau)}{\sinh\{n\Gamma_o^{-1}(1 + \sigma)\cosh(\sigma/\sigma_o)\}} \quad , \qquad \pi/2 \leq \sigma \leq \sigma_s \quad \text{(B8b)}$$

$$= \frac{2}{\Delta} \frac{I_1(\Delta)}{I_o(\Delta)} \{\exp[-(\sigma_o/\Gamma_o)\sinh(\sigma/\sigma_o)]\}\sin(\tau) \, , \qquad \sigma_s \leq \sigma \leq \infty \quad \text{(B8c)}$$

where $\Delta = (2/\Gamma_o)\cosh(\sigma_s/\sigma_o)$ (B9)

and the 'scaled' shock-termination distance σ_s is obtained by solving

transcendental equation, previously expressed by the author[40] in slightly different form for plane or spherical waves as,

$$\left(\frac{1}{\sigma_o} + \frac{\sigma_s}{\sigma_o}\right) \cosh(\sigma_s/\sigma_o) = \left(\alpha_o r_o\right)^{-1}. \tag{B10}$$

By varying σ_o we can compute σ_s/σ_o for particular values of $\alpha_o r_o$, evaluate Δ via Equation (B9) and thus obtain the total finite-amplitude absorption loss $EXDB_\infty$ for Equation (B8c) in the form,

$$EXDB_\infty = 20 \operatorname{Log}_{10}\left\{\frac{2}{\Delta} \frac{I_1(\Delta)}{I_o(\Delta)}\right\} . \tag{B11}$$

Values of $EXDB_\infty$ obtained in the manner are found to be in good agreement with similar values calculated with the aid of Equation (31b).

References

1. P. J. Westervelt, J. Acoust. Soc. Amer. 29, 199-203 (1957); 29, 934-935 (1957.

2. P. J. Westervelt, J. Acoust. Soc. Amer. 32: 934 (A) - 1960.

3. L. D. Landau and E. M. Lifshitz, "Theory of Elasticity," (Addison-Wesley, New York, 1964), pp. 115-117.

4. P. J. Westervelt, J. Acoust. Soc. Amer. 35, 535-537 (1963).

5. A. I. Eller, J. Acoust. Soc. Amer. 56, 1735-1739 (1974).

6. H. M. Merklinger, J. Acoust. Soc. Amer. 58, 784-787 (1975).

7. H. O. Berktay, J. Sound Vib. 2, 435-461 (1965).

8. M. B. Moffett, P. J. Westervelt, and R. T. Beyer, J. Acoust. Soc. Amer. 47, 1473-1474 (L) (1970); 49, 339-343 (1971).

9. H. O. Berktay, J. Sound Vib. 2, 462-470 (1965).

10. H. O. Berktay and C. A. Al-Temimi, J. Sound Vib. 9, 295-307 (1969).

11. H. O. Berktay and C. A. Al-Temimi, J. Sound Vib. 13, 67-88 (1970).

12. H. O. Berktay and C. A. Al-Temimi, J. Acoust. Soc. Amer. 50, 181-187 (1971).

13. G. R. Barnard, J. G. Willette, J. J. Truchard, and J. A. Shooter, J. Acoust. Soc. Amer. 52, 1437-1441 (1972).

14. H. O. Berktay and T. G. Muir, J. Acoust. Soc. Amer. 53, 1377-1383 (1973).

15. P. H. Rogers, A. L. Van Buren, A. O. Williams Jr., and J. M. Barber, J. Acoust. Soc. Amer. 55, 528-534 (1974).

16. J. J. Truchard, in "Finite-Amplitude Wave Effects in Fluids," L. Bjørnø Ed. (IPC Science and Technology Press Ltd., Guildford, Surrey, England, 1974) pp. 184-189.

17. T. G. Goldsberry, J. Acoust. Soc. Amer. 56: S41 (A) - 1974.

18. R. N. McDonough, J. Acoust. Soc. Amer. 57, 1150-1155 (1975).

19. J. F. Bartram, J. Acoust. Soc. Amer. 55: S23 (A) - 1974.

20. V. P. Kuznetsov, Sov. Phys. Acoust. 16, 467-470 (1971).

21. E. A. Zabolotskaya and R. V. Khokhlov, Sov. Phys. Acoust. 15, 35-40 (1969).

22. E. A. Zabolotskaya and R. V. Khokhlov, Sov. Phys. Acoust. 16, 39-42 (1970).

23. O. V. Rudenko, S. I. Soluyan and R. V. Khokhlov, Sov. Phys. Acoust. 19, 556-559 (1974).

24. D. T. Blackstock, J. Acoust. Soc. Amer. 36, 217-219 (L) (1964).

25. J. M. Burgers, Adv. Appl. Mechanics 1, 171-199 (1948).

26. P. M. Morse and H. Feshbach, "Methods of Theoretical Physics" (McGraw Hill, New York, 1953) pp. 784-785.

27. J. A. Shooter, T. G. Muir and D. T. Blackstock, J. Acoust. Soc. Amer. 55, 54-62 (1974).

28. R. Bellman, S. P. Azen and J. M. Richardson, Q. Appl. Math. 23, 55-67 (1965).

29. F. H. Fenlon and W. Kesner, "Nonlinear Scaling Laws for Parametric Receiving Arrays, Part II: Numerical Analysis," Westinghouse Electric Corporation, 1976.

30. F. H. Fenlon, in "Finite-Amplitude Wave Effects in Fluids," L. Bjørnø Ed. (IPC Science and Technology Press Ltd., 1974) pp. 160-167.

31. H. M. Merklinger, J. Acoust. Soc. Amer. 54, 1760-1761 (L) (1973).

32. H. M. Merklinger, R. H. Mellen and M. B. Moffett, J. Acoust. Soc. Amer. 53, 383 (A) - 1973.

33. F. Bowman, "Introduction to Bessel Functions" (Dover Publications Inc., New York, 1958) p. 78.

34. D. T. Blackstock, J. Acoust. Soc. Amer. 36, 534-542 (1964).

35. E. Fubini, Alta Frequenza 4, 530-581 (1953).

36. D. T. Blackstock, J. Acoust. Soc. Amer. 39, 1019-1026 (1966).

37. R. D. Fay, J. Acoust. Soc. Amer. 3, 222-241 (1931).

38. K. A. Naugol'nykh, S. I. Soluyan and R. V. Khokhlov, Sov. Phys. Acoust. 9, 42-46 (1963).

39. B. Cary, J. Acoust. Soc. Amer. 42, 88-92 (1967).

40. F. H. Fenlon, J. Acoust. Soc. Amer. 50, 1299-1312 (1971).

41. F. H. Fenlon, J. Acoust. Soc. Amer. 56: S41 (A) - 1974.